Journal of Geosciences, Osaka City University
Vol. 54, Art. 1, p. 1-16, March, 2011

Petrography and Geochemistry of the Lower Paleozoic Araba Formation, Northern Eastern Desert, Egypt: Implications for Provenance, Tectonic Setting and Weathering Signature

Hossam A. TAWFIK[1], Ibrahim M. GHANDOUR[2], Wataru MAEJIMA[1], and Abdel-Monem T. ABDEL-HAMEED[3]

[1] Department of Geosciences, Graduate School of Science, Osaka City University, Sumiyoshi-ku, Osaka 558-8585, Japan, E-mail: hossam@sci.osaka-cu.ac.jp; maejima@sci.osaka-cu.ac.jp
[2] Department of Marine Geology, Faculty of Marine Sciences, King Abdul Aziz University, 80207 Jeddah 21589, Saudi Arabia, E-mail: ighandour@kau.edu.sa
[3] Department of Geology, Faculty of Science, Tanta University, Tanta 31527, Egypt, E-mail: hatabdelhameed@yahoo.com

Abstract

This study focuses on the Lower Paleozoic sandstones of the Araba Formation exposed in the northern Eastern Desert, Egypt, to identify the possible source, geotectonic setting, and weathering effects using integrated petrographical and geochemical approaches. Modal petrographic analyses revealed that the sandstones are mainly diagenetic quartzarenites. The Araba framework composition indicated that the source area comprises plutonic igneous and metamorphic rocks of cratonic interior and recycled orogenic settings. Geochemically, these sandstones are commonly enriched in SiO_2, Ba, Sr, and Zr indicating their derivation from felsic granitic-gneissic terrain. They are characterized by a lower Fe_2O_3*+MgO and Al_2O_3/SiO_2, as well as elevated $K_2O/Na_2O>>1$ and $Al_2O_3/(CaO+Na_2O)$ ratios pointing to a passive continental margin deposition. Increased Chemical Index of Alteration (CIA) and Plagioclase Index of Alteration (PIA) values indicate that these deposits were subjected to a significant chemical weathering at the source area and intensive alteration and removal of alkalis during diagenesis. The high chemical maturity has resulted from widespread chemical weathering of the Pan-African continental Precambrian rocks. Moreover, this study clarifies that a warm-humid paleoclimate has prevailed over northern Egypt in the aftermath of the Pan-African Orogeny.

Key-words : Araba Formation, Egypt, Geochemistry, Provenance, Chemical weathering

Introduction

The chemical composition of terrigenous sedimentary rocks is a function of the complex interplay of various variables, such as provenance, weathering, transportation, and diagenesis (Bhatia, 1983). Recent investigations on geochemical characteristics of ancient and modern detritus have been carried out in order to infer the source rocks, provenance, and tectonic setting (e.g., Potter, 1978; Bhatia, 1983; Bhatia and Crook, 1986; Roser and Korsch, 1986; 1988; McLennan et al., 1993).

Provenance studies serve to reconstruct the predepositional history of a sediment or sedimentary rock. This includes the distance and direction, size and setting of the source region, climate and relief in the source area, and

the specific type of sedimentary rocks (Pettijohn et al., 1987; McCann, 1998), geochemical features (Bhatia and Crook, 1986; Roser and Korsch, 1988; Armstrong-Altin et al., 2004), and heavy mineral assemblages (Chaodong et al., 2005).

Lower Paleozoic successions in the Gulf of Suez province and at the northeastern part of Egypt, were extensively studied from the lithostratigraphic and chronological points of view (e.g. Issawi and Jux, 1982; El Shahat and Kora, 1986; El Kelani and Said, 1989; Kora, 1991; Abdallah et al., 1992). Due to their economic significance, many publications were dealt with petrographic characteristics, diagenetic evolution, and reservoir quality and heterogeneity of these rocks (e.g., Tawfik et al., 2009; Tawfik et al., 2010). However, other studies were performed on the depositional setting of these sediments (e.g. Ahmed and Osman, 1998; El Araby and Abdel-Motelib, 1999; Ghandour et al., 2009). Thus far there have been no attempts made on the Araba Sandstone in the northern Eastern Desert of Egypt to declare the major and trace element geochemistry of these sandstones in order to infer their provenance, tectonic setting, and weathering signature.

Geological Background

The investigated area, Gebel Somr El-Qaa, is located to the west of the Gulf of Suez, in the northern Eastern Desert, Egypt (Fig. 1). In this area, the Precambrian crystalline rocks are nonconformably overlain by the Cambro-Ordovician sandstones of the Araba and Naqus formations, respectively (Fig. 1), followed by a thick marine sequence of Late Cretaceous to Eocene age (Abdallah et al., 1992). At this area, the Lower Paleozoic Araba Formation consists entirely of fine- to coarse-grained sandstone, with subordinate pebbly sandstone and sandy mudstone intercalations. Conglomeratic beds are restricted to the lower part of the succession (Fig. 2). The Araba Formation varies in thickness from 120 m at the type locality, Gebel Araba, SW Sinai (Said, 1971) to about

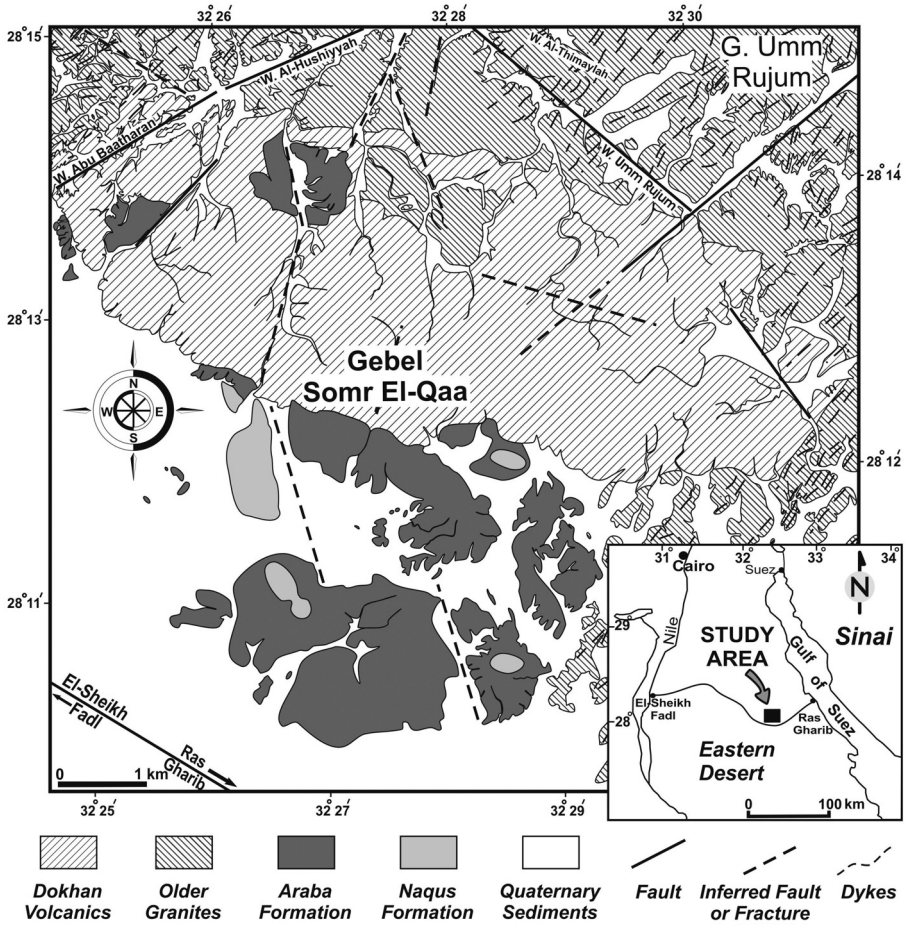

Fig. 1 Geological map of Somr El-Qaa area, northern Eastern Desert, Egypt.

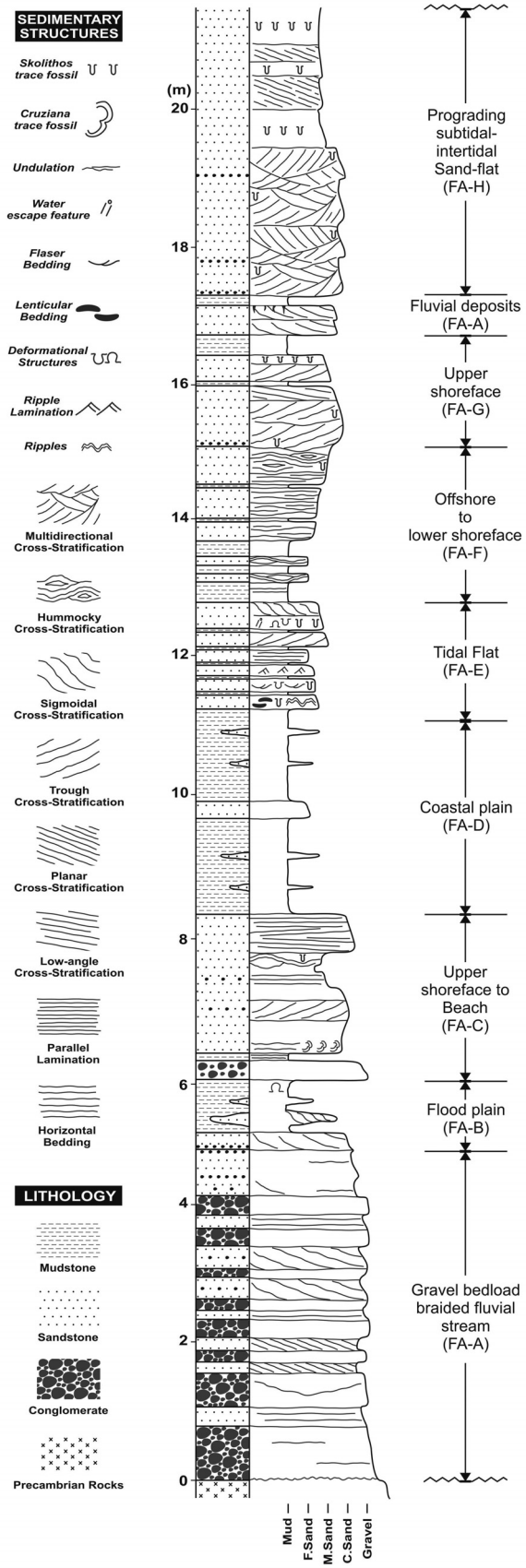

Fig. 2 A simplified stratigraphic succession of the Lower Paleozoic Araba Formation at the study area. Depositional facies are modified after Ghandour et al. (2009).

25 m at the area of Gebel Somr El-Qaa (Ghandour et al., 2009) depending on the location of irregular surface over which deposition took place. The rocks exhibit variable colours from reddish brown, pinkish brown to pale pink and grayish white. Most of the sandstones are highly cemented by reddish Fe-oxides staining and whitish kaolinite and quartz cements, whereas rare horizons are friable to poorly-cemented. The trace fossils, *Skolithos linearis* and less abundant *Cruziana salomonis*, are the most identified ichnofossils. Ghandour et al. (2009) subdivided the Araba Formation exposed at the study area into three depositional sequences (SQ 1 - SQ 3) which are differentiated into eight facies assemblages (FA-A to FA-H) ranging from fluvial, transitional to shallow-marine settings (Fig. 2).

The Araba Formation (Said, 1971) seems to be barren of body fossils, and as a result, precise biostratigraphic determinations are quite impossible (Sabaou et al., 2009). It has been assigned to the Early Cambrian (Seilacher, 1990) to Cambro-Ordovician (El-Shahat and Kora, 1986; Abdallah et al., 1992) and to Cambrian (Said and El Kelani, 1988) (Table 1). The Araba Formation is coeval to the Lower Sandstone Series of Barron (1907) and the Lower Yam Suf Group of Weissbrod (1969). In addition, it is equivalent to the Sarabit El Khadim, Abu Hamata, and Adedia formations of Soliman and El-Fetouh (1969); to the Sarabit El-Khadim, Abu Hamata, Nasib, and Adedia formations of El Shahat and Kora (1986); and also to the Amudei Shelomo, Timna and Shehoret formations of Weissbrod and Perath (1990). In the subsurface of the Gulf of Suez region, the Araba Formation is equivalent to the informal Nubian D (Klitzsch, 1990; Alsharhan and Salah, 1997) (Table 1).

Analytical Techniques

Four stratigraphic sections were measured from the area of Gebel Somr El-Qaa. A total of 33 sandstone samples were selected for petrographic analyses (Table 2). The sandstone modal composition was quantified based on counting 500 points using the Gazzi-Dickinson method as described by Ingersoll et al. (1984).

Clay mineralogy was determined by X-ray diffraction analysis on 26 powdered samples, using both smear-on glass slide and powder press techniques (Hardy and Tucker, 1988). The analysis was done by a RIGAKU RAD-I X-ray diffractometer (CuKα-radiation with 30 kV, 10 mA, 2°-70° 2-theta). Discrimination between kaolinite and chlorite was done after heating the samples to 550℃ for two hours in a muffle furnace (Tucker, 1988). Peak locations and intensities were determined digitally using

Diffrac/AT software, and minerals were identified by their characteristic reflections (Moore and Reynolds, 1989). Furthermore, twenty samples were gold-coated and examined under the scanning electron microscope (KEYENCE VE-7800), at 20 kV accelerating voltage for identification of delicate diagenetic cements.

Major and trace elements composition of 32 sandstone samples were determined by a RIGAKU RIX 2100 X-ray fluorescence spectrometer (XRF), equipped with Rh/W dual-anode X-ray tube. The analyses were performed on the whole rock specimens under 50 kV and 50 mA accelerating voltage and tube current, respectively. Fused glass beads were prepared by mixing 1.8 gm of powdered sample (dried to 110℃ for 4 hours), 3.6 gm of spectroflux

Table 1 Lithostratigraphic subdivisions of the Lower Paleozoic rocks in Northern Egypt and Israel.

1	2	3	4	5	6
Somr El-Qaa, N Eastern Desert	***Um Bogma, SW Sinai***		***Taba, NE Sinai***	***Timna, Israel***	***Gulf of Suez***
(Ordov. ?) Naqus Fm.	Carboniferous: Adedia Fm.	Cambro-Ordovician: Adedia Fm.	Cambrian: Naqus Fm.	Cambrian: Netafim Fm.	Cambrian: Nubian C
Cambro-Ordovician: Araba Fm.	Abu Hamata Fm.	Nasib Fm. / Abu Hamata Fm.	Araba Fm.	Shehoret Fm. / Timna Fm.	Nubian D
	Sarabit El-Khadim Fm.	Sarabit El-Khadim Fm.	Taba Fm.	Amudei Shelomo Fm.	

1: Abdallah et al. (1992); **2**: Soliman and El-Fetouh (1969); **3**: El Shahat and Kora (1986); **4**: Said and El Kelani (1988); **5**: Weissbrod and Perath (1990); **6**: Klitzsch (1990) and Alsharhan and Salah (1997).

Table 2 Modal analysis data presenting composition of the Araba sandstones.

Sample No.	Detrital Mineralogy							Cementing Material							Porosity	Present Composition			IGV	MI
	Qm	Qp	Qt	FD	RF	M	HM	Ka	Fe	Qz	Cl	Ha	TPC	TRC		Q	F	L		
AR 33	44.5	9.1	53.6	0.0	0.2	1.0	1.5	5.8	4.1	11.8	1.9	0.0	23.5	1.3	18.9	99.6	0.0	0.4	33.5	99.6
AR 32	40.5	5.6	46.1	0.2	0.0	3.7	1.4	11.6	5.4	6.2	3.7	0.0	26.8	3.3	18.5	99.6	0.4	0.0	39.8	99.6
AR 31	42.7	10.7	53.4	0.2	0.6	3.5	1.6	8.5	24.3	0.6	1.0	0.0	34.4	1.4	5.1	98.6	0.4	1.1	37.9	98.6
AR 30	40.3	5.4	45.7	0.0	3.1	7.9	0.8	5.7	31.9	0.6	1.2	0.0	39.4	0.2	3.0	93.7	0.0	6.3	42.4	93.7
AR 29	47.3	10.1	57.4	0.0	4.0	1.2	2.0	11.3	7.1	2.0	4.6	0.0	25.0	0.4	10.1	93.5	0.0	6.5	32.9	93.5
AR 28	54.0	7.9	61.9	0.0	1.0	0.8	0.4	9.1	6.9	2.6	4.3	0.0	22.9	1.2	11.9	98.4	0.0	1.6	32.4	98.4
AR 27	49.0	13.0	62.0	0.2	0.4	0.4	0.8	2.5	1.0	8.8	1.5	0.0	13.8	0.0	22.6	99.1	0.3	0.6	27.3	99.1
AR 26	45.2	5.3	50.5	0.0	1.4	0.6	0.2	6.5	3.4	10.1	2.2	0.0	22.1	0.4	24.9	97.3	0.0	2.7	34.1	97.3
AR 25	45.8	12.8	58.5	0.2	0.0	2.2	1.0	11.2	2.4	5.3	2.2	0.0	21.0	1.2	15.9	99.7	0.3	0.0	30.3	99.7
AR 24	55.1	8.1	63.2	0.0	0.6	0.2	0.6	2.4	2.0	17.7	0.0	0.0	22.0	0.0	13.4	99.1	0.0	0.9	33.1	99.1
AR 23	42.8	7.0	49.8	0.4	4.3	0.2	0.6	5.6	0.6	10.9	1.6	0.0	18.7	0.6	25.5	91.4	0.7	7.9	28.6	91.4
AR 22	42.2	3.7	45.9	0.2	3.1	0.8	0.2	10.3	2.0	7.4	2.1	0.0	21.8	0.8	27.2	93.3	0.4	6.3	31.1	93.3
AR 21	36.8	8.8	45.7	0.0	8.5	1.0	0.6	13.7	3.2	2.3	2.6	0.0	21.8	0.0	22.6	84.4	0.0	15.6	28.8	84.4
AR 20	33.9	18.3	52.1	0.0	5.6	4.3	0.2	10.1	22.6	0.4	1.0	0.0	34.1	1.9	1.8	90.2	0.0	9.8	34.2	90.2
AR 19	38.9	10.1	49.0	0.0	7.3	4.4	0.4	16.3	9.9	0.8	5.4	0.0	32.4	2.0	4.6	87.0	0.0	13.0	35.7	87.0
AR 18	35.2	7.7	42.8	0.0	6.9	0.2	0.4	11.6	6.3	9.6	5.9	0.0	33.4	0.4	15.9	86.2	0.0	13.8	42.6	86.2
AR 17	47.1	9.2	56.3	0.2	3.9	0.4	1.4	8.3	4.2	12.3	0.2	0.0	25.0	1.0	11.9	93.3	0.3	6.4	31.5	93.3
AR 16	39.4	9.7	49.1	0.0	2.8	1.2	0.4	13.6	7.7	6.3	2.8	0.0	30.4	1.6	14.6	94.7	0.0	5.3	42.6	94.7
AR 15	37.4	7.0	44.4	0.0	9.3	1.7	0.4	18.5	4.5	7.6	2.3	0.0	32.9	1.2	10.1	82.6	0.0	17.4	39.7	82.6
AR 14	36.2	5.7	42.0	0.0	2.1	0.8	1.0	9.0	1.3	8.2	1.9	0.0	20.5	0.2	33.5	95.2	0.0	4.8	39.5	95.2
AR 13	47.4	8.4	55.8	0.0	6.4	2.4	0.2	8.8	17.1	2.2	1.0	0.0	29.1	1.0	5.2	89.8	0.0	10.2	32.3	89.8
AR 12	45.1	6.0	51.1	0.0	0.4	5.4	0.2	18.2	14.6	1.4	1.6	0.0	35.7	2.0	5.2	99.2	0.0	0.8	40.9	99.2
AR 11	27.2	17.1	44.2	0.0	2.4	7.9	0.0	7.9	32.7	0.0	0.0	0.0	40.7	2.6	2.2	94.9	0.0	5.1	42.5	94.9
AR 10	36.0	11.6	47.6	15.9	0.8	4.3	0.6	10.8	5.1	0.2	0.2	0.0	16.4	2.0	12.4	74.0	24.8	1.2	26.4	74.0
AR 09	40.5	16.2	56.7	0.0	10.5	0.2	0.2	14.3	3.7	2.3	0.0	0.0	20.3	1.4	10.8	84.4	0.0	15.6	25.9	84.4
AR 08	38.2	17.9	56.0	0.0	19.7	0.1	0.1	10.5	3.0	1.8	1.6	0.0	16.9	0.6	6.6	74.0	0.0	26.0	19.4	74.0
AR 07	41.1	20.1	61.2	0.0	16.0	0.2	0.2	11.9	2.4	0.6	0.6	0.0	15.4	0.2	6.7	79.2	0.0	20.8	19.2	79.2
AR 06	45.1	14.9	60.0	0.3	6.3	0.4	0.5	16.9	0.0	4.1	0.6	0.0	21.6	0.8	10.2	90.1	0.4	9.4	27.8	90.1
AR 05	35.5	19.2	54.7	0.0	22.2	0.2	0.0	6.7	0.0	1.0	1.6	0.0	9.2	0.2	13.5	71.1	0.0	28.9	17.4	71.1
AR 04	39.4	13.2	52.6	0.0	14.4	0.0	0.0	18.6	0.8	1.0	1.8	0.0	22.2	0.6	10.3	78.5	0.0	21.5	28.3	78.5
AR 03	40.8	10.4	51.1	0.8	16.8	1.2	0.2	10.3	1.0	1.2	1.0	0.0	13.4	1.0	15.6	74.4	1.1	24.4	22.8	74.4
AR 02	32.9	5.9	38.8	13.3	10.9	1.0	0.2	14.3	0.0	2.2	0.0	0.0	16.4	6.2	13.3	61.6	21.1	17.3	20.2	61.6
AR 01	30.0	6.9	36.9	20.7	4.5	3.0	0.6	15.2	2.6	3.0	0.0	6.1	26.8	2.8	4.7	59.4	33.3	7.3	30.2	59.4
Average	41.0	10.4	51.4	1.6	5.9	1.9	0.6	10.8	7.1	4.6	1.8	0.2	24.4	1.2	13.0	87.2	2.7	10.1	31.9	87.2

Explanation: *Qm*, Monocrystalline Quartz; *Qp*, Polycrystalline Quartz; Qt, Total Quartz; *FD*, Feldspar; *RF*, Rock Fragment; *M*, Mica; *HM*, Heavy Minerals; Ka, Kaolinite Cement; Fe, Iron-oxides Cement; *Qz*, Quartz Cement; *Cl*, Calcite Cement; *Ha*, Halite Cement; *TPF*, Total Pore-filling Cement; *TRC*, Total Replacement Cement (calcite and Kaolinite); *Q*, Quartz; *F*, Feldspar; *L*, Lithic fragment; *IGV*, Intergranular volume; *MI*, Maturity Index.

($Li_2B_4O_7$ 20%, $LiBO_2$ 80%, dried at 450℃ for 4 hours), 0.54 gm of oxidant $LiNO_3$ (dried at 110℃ for 4 hours) and traces of LiI. The mixture is fused at 800℃ for 120 sec and 1200℃ for 200 sec, based on the method of Furuyama et al. (2001). Both the Chemical Index of Alteration (CIA) and Plagioclase Index of Alteration (PIA) were calculated for the studied samples using the method of Nesbitt and Young (1982) and Fedo et al. (1995), respectively. The indices represent the molar ratios of $[Al_2O_3/(Al_2O_3+CaO^*+K_2O+Na_2O)]\times100$ and $[(Al_2O_3-K_2O)/(Al_2O_3+CaO^*+Na_2O-K_2O)]\times100$, respectively. All the mineralogical and chemical analyses were undertaken by the corresponding author at the Department of Geosciences, Osaka City University.

Results

Petrography

The Araba sandstones vary from very fine- to very coarse-grained and from poorly- to very well-sorted with heterogeneous roundness of grains. Three architectural components, framework grains (av. 61.4%), cementing materials (av. 25.6%), and porosities (av. 13%), are determined (Table 2). The detrital mode is dominated by quartz, with variable amounts of lithic grains, minor feldspar, and accessory mica and heavy minerals. Quartz population is dominated by monocrystalline quartz (Qm), averaging 41%, and mostly exhibit nonundulose to slightly undulose extinctions. Quartz grains sometimes include inclusions such as zircon and tourmaline. Polycrystalline grains (Qp) are next in abundance (av. ~10%); almost all types described by Blatt (1992) are observed in the Araba sandstones. The most important are: 1) polycrystalline with two to five subcrystals and straight to slightly-curved intercrystalline boundaries; 2) those with elongated five or more crystals with sutured and crenulated intercrystalline subcrystal boundaries (Fig. 3A); and 3) grains with great variation in crystal sizes "bimodal distribution" (Fig. 3B).

Feldspar occurs in the lower part of the succession at certain horizons, averaging 1.6% and is dominated by K-feldspars such as microcline and less abundantly plagioclases (Fig. 3C). Most of the feldspar grains are altered to kaolinite and illite. The presence of altered feldspar, grain-like patches of kaolinite, and oversized

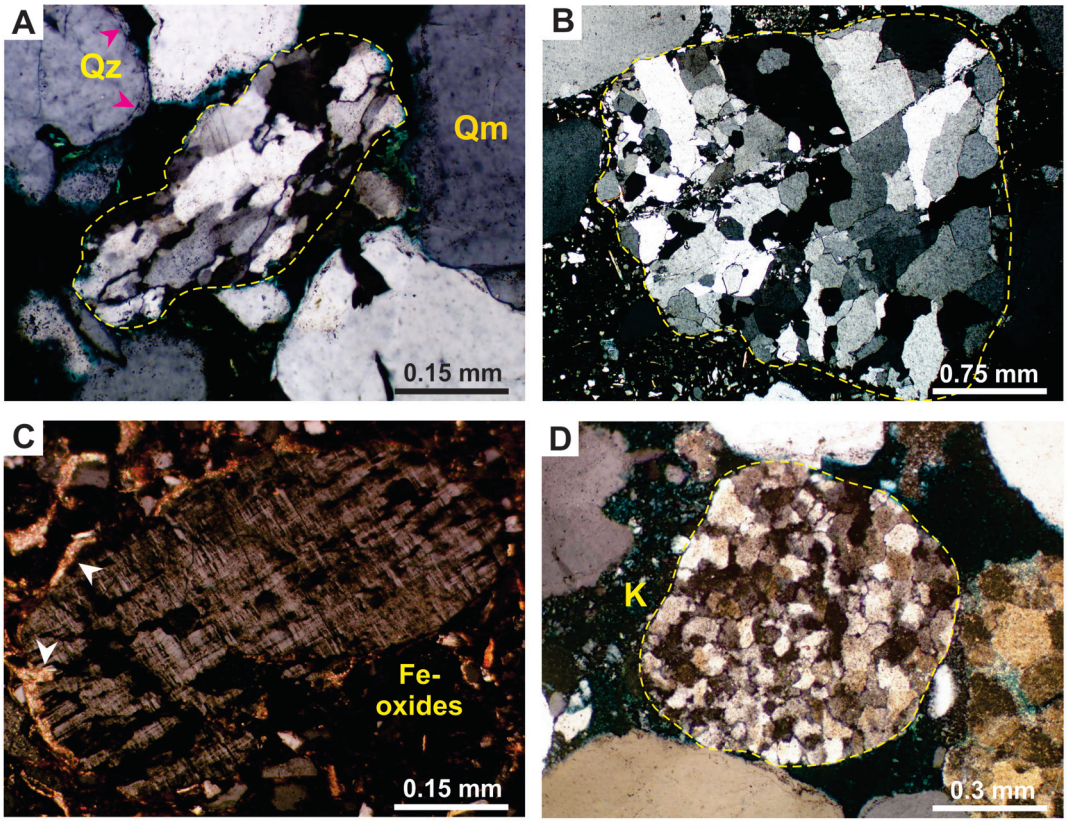

Fig. 3 Photomicrographs of the Araba sandstones showing: (A) polycrystalline quartz grain consisting of elongated subcrystals with sutured and crenulated intercrystalline boundaries. Arrows refer to quartz overgrowth (Qz) around monocrystalline quartz (Qm); (B) polycrystalline quartz grain displaying a bimodal size distribution of subcrystals; (C) unaltered detrital microcline feldspar embedded in reddish iron-oxide cement. Note the replacement of feldspar grain by calcite cement (arrows); (D) coarse-grained metamorphic quartzite fragment surrounded by kaolinite cement (K).

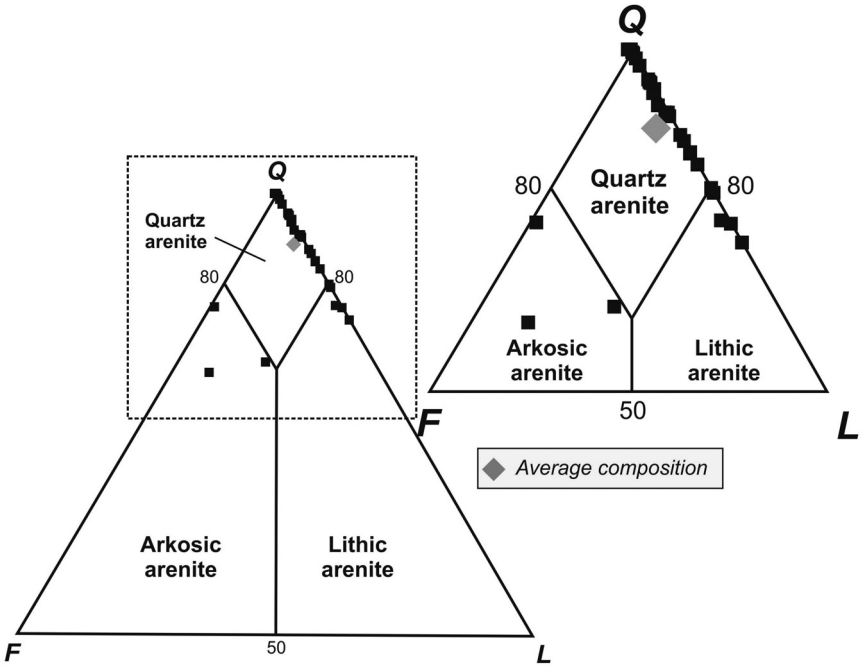

Fig. 4 QFL diagram after Pettijohn et al. (1987).

pores indicate that the feldspar content in the original framework composition were higher at the time of deposition.

Lithic fragments are the second most abundant component (av. ~6%) next to quartz. They include many varieties such as metamorphic fragments (Lm) consisting of quartzite, schist and gneiss (Fig. 3D), sedimentary lithic grains (Ls) including microcrystalline chert, and igneous fragments (Li) made up of felsic granites.

Muscovite is the most common accessory mineral, averaging 2%, and is an important component in fine-grained sandstones. Heavy minerals comprise a minor constituent (<1%) of the bulk composition and are exclusively dominated by the ultrastable ZTR group. Compositionally, the Araba sandstones are classified as quartz arenite (Pettijohn et al., 1987), with variable amounts of lithic arenite and arkosic arenite (Fig. 4). Their average framework composition is $Q_{87}F_3L_{10}$.

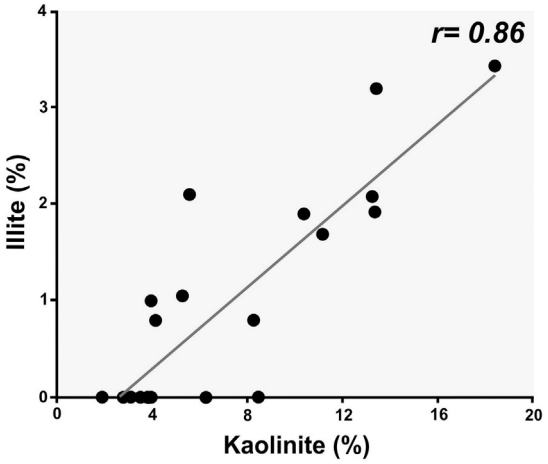

Fig. 5 A positive relationship between kaolinite and illite clay minerals.

Clay mineralogy

X-ray diffraction analysis showed that kaolinite and illite are the only clay mineral species detected in the Araba sandstones. Kaolinite occurs in almost all the studied samples. As evident from thin section examination, the relative abundance of kaolinite decreases from the lower to the upper part of the formation due to upward decrease in feldspar content. Illite is the other abundant clay mineral. Its vertical distribution coincides with that of kaolinite throughout the formation (Fig. 5). In fine-grained sandstones, illite assumes greater importance; this is probably due to the abundance of mica polymorph. The positive correlation between kaolinite and illite clay minerals with other non-clay minerals except quartz, in addition to their high degree of crystallinity, as well as the euhedral shape of kaolinite as confirmed by SEM study (Fig. 6A), support the authigenic origin of clay minerals.

Diagenetic impact

Compaction, cementation, dissolution, and

replacement are the most important diagenetic modifications noticed in the Araba sandstones. Compactional effects are expressed by: 1) three to four contacts per grain; 2) numerous squeezed lithoclasts; 3) bending of muscovite; and 4) fractured quartz and rock fragments. Chemical compaction has resulted in the development of long and concavo-convex contacts, and less commonly sutured contact.

Cementing materials include clay minerals, iron-oxides, quartz and calcite cements, together with traces of gypsum and halite. Kaolinite is the most abundant (av. 10.8%; Table 2), followed by a minor amount of illite. Kaolinite occurs mainly as face-to-face stacking pseudohexagonal platelets and vermicular crystals (Fig. 6A), whereas illite exhibits delicate fibrous lathes and pore-bridges. Kaolinite is mostly derived from the alteration of detrital feldspars as indicated by abundant, kaolinite-replaced feldspars (Fig. 6A). However, with increasing burial (~ 2.5 km) the presence of excess K-feldspar leads to kaolinite transformation into illite. Iron-oxides are the second most abundant cements (av. 7.1%; Table 2) and are represented by hematite and goethite as detected by XRD analysis and optical microscopy. Fe-oxide cements are intergrown with clays and sometimes rimming or form thick coating (~5 μm) around detrital grains reducing primary and secondary porosities. Hematite occurs as micro-rosettes, whereas goethite exhibits tiny acicular crystals that are associated with hematite. Iron was probably released by the breakdown of unstable Fe-bearing minerals such as biotite and amphiboles within the sediment.

Quartz overgrowth constitutes a considerable amount in the Araba sandstones (av. 4.6%; Table 2) and occurs as euhedral and syntaxial overgrowths around detrital quartz grains (Fig. 3A). Less commonly, quartz cement exhibits microcrystalline crystals, growing as a multitude of crystals, 10 - 20 μm in length. The silica required for the formation of quartz overgrowths was probably derived from the alteration of detrital feldspar and intergranular pressure dissolution.

Calcite cements are minor (av. 1.8%; Table 2), and they occur as patchy distribution in some thin sections. Two types of calcite are observed: 1) fine microspar and fringe crystals, and 2) poikilotopic coarser calcite fabric (Fig. 6B). The former was probably formed from meteoric water at shallow burial, whereas the latter was precipitated

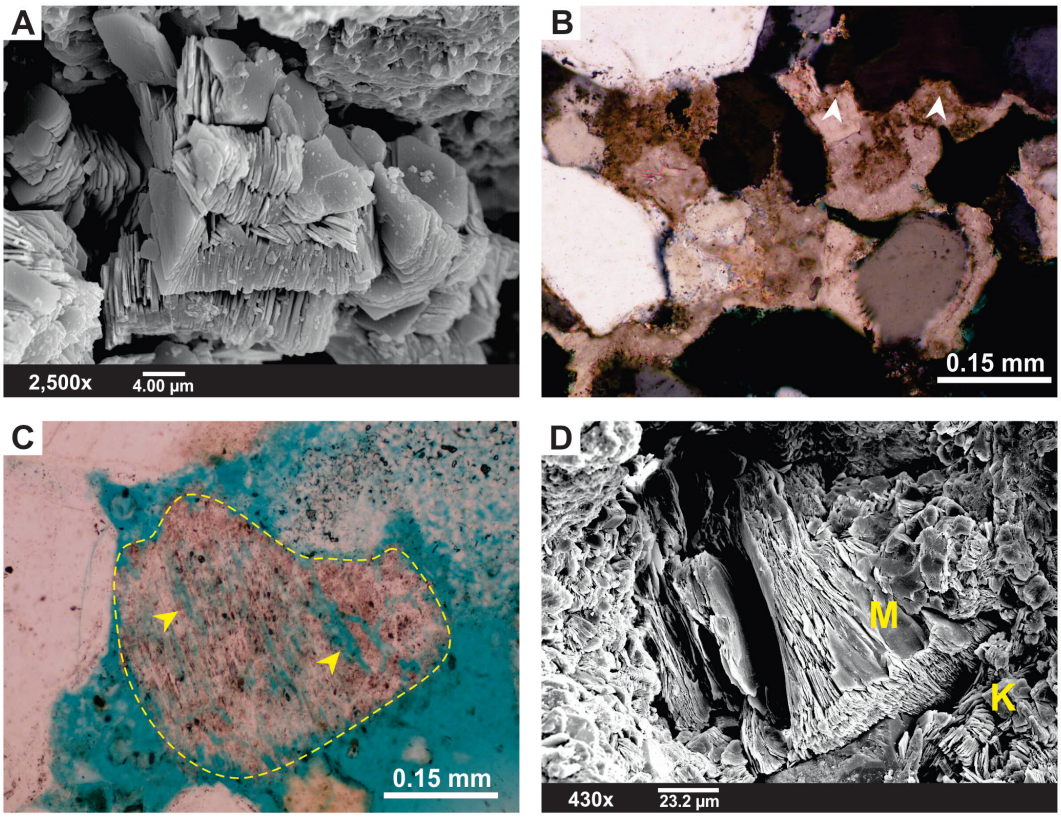

Fig. 6 (A) SEM image of vermicular kaolinite; (B) Photomicrograph of poikilotopic calcite cement. Note the embayment (arrows) within quartz grains; (C) Optical photograph of partly dissolved K-feldspar grain with abundant intraporosities (strained blue, arrows); (D) SEM image showing early-stage replacement of muscovite flakes (M) by authigenic kaolinite (K).

due to elevated temperature at greater burial depths (Salem et al., 1998). Traces of gypsum and halite cements are also detected. These evaporative phases may be released by modern meteoric water from nearby Miocene outcrops and later precipitated by evaporation in low areas where the Araba sandstones are present.

Dissolution process has led to development of secondary porosity. The majority of dissolved grains were probably feldspars (Fig. 6C) although labile rock fragments and mafics, as well as unstable heavy minerals were also suffered from dissolution effects. Calcite cement is also suffered from dissolution process as indicated by the presence of moldic pores rimmed by calcite cement and high values of intergranular volume (IGV). Calcite is

Table 3 Major and trace elements composition of the studied sandstones.

Oxides (Wt %)	AR 01	AR 02	AR 03	AR 04	AR 05	AR 08	AR 09	AR 10	AR 11	AR 12	AR 13	AR 14	AR 15	AR 16	AR 17	AR 18
SiO_2	68.05	81.86	92.19	94.22	88.87	94.07	84.02	78.62	74.86	78.40	71.43	82.73	85.06	86.90	92.21	86.77
TiO_2	0.20	0.16	0.11	0.14	0.19	0.11	0.24	0.16	0.52	0.44	0.67	0.20	0.14	0.16	0.09	0.26
Al_2O_3	7.01	10.05	3.80	4.62	5.95	4.33	6.50	10.41	13.35	13.44	15.07	8.34	8.02	8.10	3.67	6.67
Fe_2O_3	0.36	0.45	0.49	0.26	0.33	0.47	0.62	1.39	4.13	1.62	4.52	0.53	0.63	0.43	0.30	0.58
MnO	0.01	0.01	0.00	0.00	0.00	0.00	0.00	0.01	0.01	0.01	0.02	0.01	0.01	0.00	0.00	0.01
MgO	0.09	0.20	0.15	0.15	0.15	0.10	0.21	0.27	0.13	0.10	0.23	0.32	0.08	0.16	0.09	0.11
CaO	0.13	0.18	0.51	0.52	0.37	0.20	1.38	0.58	0.06	0.06	0.26	1.10	0.45	0.38	1.07	1.36
Na_2O	5.56	0.15	0.03	0.03	0.11	0.07	0.09	0.13	0.05	0.01	0.02	0.04	0.68	0.04	0.04	0.01
K_2O	2.03	2.35	0.26	0.31	0.42	0.30	0.40	3.61	0.33	0.21	0.56	0.24	0.08	0.08	0.06	0.05
P_2O_5	0.05	0.08	0.04	0.03	0.04	0.02	0.03	0.10	0.14	0.08	0.18	0.05	0.03	0.04	0.07	0.03
Total	83.48	95.49	97.58	100.28	96.42	99.67	93.50	95.28	93.57	94.37	92.95	93.56	95.16	96.29	97.60	95.83
SiO_2/Al_2O_3	9.7	8.1	24.2	20.4	14.9	21.7	12.9	7.6	5.6	5.8	4.7	9.9	10.6	10.7	25.1	13.0
K_2O/Na_2O	0.4	15.3	10.0	11.6	3.8	4.2	4.4	27.0	6.6	42.0	24.4	5.6	0.1	1.9	1.8	6.6
$Fe_2O_3^*$+MgO	0.4	0.7	0.6	0.4	0.5	0.6	0.8	1.7	4.3	1.7	4.8	0.9	0.7	0.6	0.4	0.7
CIA	44.1	92.3	93.9	93.7	82.0	93.4	92.6	76.2	98.6	97.5	96.7	97.0	89.6	97.4	98.5	99.3
PIA	42.4	97.5	99.2	99.1	97.6	98.1	97.8	97.7	100	99.5	99.8	99.3	90.1	98.8	99.3	99.9
Trace Elements (ppm)																
Ba	13442	300	66	78	66	148	384	2429	203	111	235	97	48	118	252	62
Cr	5	11	9	10	9	8	11	10	35	13	36	10	6	7	6	6
Cu	20	16	7	15	13	10	3	5	6	6	11	4	7	11	5	5
Nb	4	4	5	5	5	4	7	4	10	9	14	5	3	4	2	6
Ni	4	1	0	1	0	3	0	4	1	2	14	0	2	2	1	0
Pb	11	17	9	7	11	7	11	23	74	38	42	12	23	12	9	18
Rb	59	78	13	12	20	15	19	117	14	9	37	16	4	5	4	4
Sr	149	109	103	63	76	35	68	210	643	380	457	155	127	185	172	104
V	26	15	11	9	13	10	15	18	42	18	52	14	11	12	9	10
Y	7	10	9	10	12	7	12	9	15	9	61	6	5	6	6	7
Zn	13	19	8	7	12	12	14	47	17	15	112	18	17	8	6	13
Zr	103	114	93	132	204	88	223	58	205	160	402	138	89	108	89	120

Oxides (Wt %)	AR 20	AR 21	AR 22	AR 23	AR 24	AR 25	AR 26	AR 27	AR 28	AR 29	AR 30	AR 31	AR 32	AR 33	AR 34	AR 35
SiO_2	75.66	83.49	88.17	91.49	97.42	88.16	92.34	94.82	88.45	84.24	72.87	86.88	88.48	91.10	94.49	80.95
TiO_2	0.59	0.31	0.13	0.24	0.08	0.13	0.12	0.06	0.26	0.30	0.92	0.35	0.24	0.31	0.15	0.80
Al_2O_3	12.53	9.76	6.21	5.10	2.60	5.91	4.26	1.78	6.75	7.95	13.57	7.21	7.39	3.82	3.58	12.86
Fe_2O_3	3.33	0.77	0.39	0.40	0.16	0.36	0.35	0.15	0.67	1.78	4.97	0.98	0.14	0.29	0.25	0.20
MnO	0.01	0.01	0.00	0.01	0.00	0.00	0.01	0.00	0.00	0.01	0.01	0.01	0.00	0.01	0.01	0.00
MgO	0.13	0.06	0.09	0.08	0.06	0.08	0.12	0.08	0.09	0.09	0.20	0.05	0.04	0.10	0.12	0.07
CaO	0.70	0.21	0.17	0.59	0.28	0.67	0.51	0.89	0.25	0.91	1.12	0.16	0.33	1.06	0.85	0.21
Na_2O	0.01	0.02	0.06	0.01	0.06	0.02	0.00	0.06	0.01	0.01	0.02	0.01	0.08	0.11	0.04	0.06
K_2O	0.18	0.07	0.04	0.04	0.03	0.06	0.07	0.04	0.12	0.09	0.23	0.13	0.08	0.04	0.04	0.18
P_2O_5	0.06	0.07	0.03	0.02	0.02	0.03	0.03	0.03	0.04	0.02	0.16	0.10	0.05	0.03	0.06	0.05
Total	93.21	94.78	95.29	97.96	100.70	95.42	97.80	97.91	96.65	95.40	94.05	95.87	96.84	96.86	99.59	95.39
SiO_2/Al_2O_3	6.0	8.6	14.2	18.0	37.4	14.9	21.7	53.4	13.1	10.6	5.4	12.0	12.0	23.8	26.4	6.3
K_2O/Na_2O	16.7	2.9	0.6	5.1	0.5	3.1	72.0	0.6	17.1	6.1	11.3	11.8	1.0	0.3	1.1	2.8
$Fe_2O_3^*$+MgO	3.5	0.8	0.5	0.5	0.2	0.4	0.5	0.2	0.8	1.9	5.2	1.0	0.2	0.4	0.4	0.3
CIA	98.2	97.8	95.7	97.7	98.3	98.4	98.9	98.4	94.1	98.6	98.8	96.4	99.2	98.4	99.1	98.7
PIA	99.4	98.7	96.4	98.6	99.8	99.8	99.8	99.9	95.6	100	99.6	97.2	99.8	98.9	99.7	99.9
Trace Elements (ppm)																
Ba	92	45	40	34	33	48	52	49	62	257	192	183	133	39	46	70
Cr	16	9	6	6	11	7	6	6	10	9	36	10	6	11	8	18
Cu	6	7	4	4	4	3	34	3	21	11	10	6	5	6	44	10
Nb	12	7	4	6	2	4	3	2	5	6	17	7	6	7	4	17
Ni	6	3	1	2	2	2	0	1	0	7	16	6	2	2	0	2
Pb	42	27	17	12	5	13	8	8	10	47	33	26	12	14	28	19
Rb	8	4	3	3	3	4	4	3	7	5	11	6	5	3	5	8
Sr	117	306	104	71	51	75	62	88	94	407	393	474	178	97	272	131
V	37	13	10	11	5	9	10	4	12	21	57	12	14	12	11	33
Y	26	16	6	7	4	6	7	4	7	11	259	14	7	8	6	33
Zn	28	20	8	8	5	7	7	4	16	54	40	18	7	7	10	8
Zr	379	223	101	201	82	121	93	82	163	233	884	390	244	352	168	909

Explanation: *CIA*, Chemical Index of Alteration; *PIA*, Plagioclase Index of Alteration.

highly replacive to detrital grains such as quartz, feldspar, and muscovite as well as to quartz overgrowth (Fig. 6B). Muscovite is severely replaced by kaolinite cement. The replacement begins at the split end of muscovite (Fig. 6D), and proceeds leaving behind hairlets-like relics of mica swam within kaolinite booklets. For more detailed interpretation of post-depositional processes, mineral paragenesis, and diagenetic impact on reservoir quality of the Araba sandstones at Somr El-Qaa area, refer to Tawfik et al. (2009 and 2010).

Geochemistry

The data of major and trace elements analyses of the Araba sandstones are outlined below and listed in Table 3.

Major elements

The present sandstones are enriched in SiO_2 (av. 85.6%) and relatively Al_2O_3 (av. 7.5%) and depleted in TiO_2 (av. 0.3%), Fe_2O_3 (av. 1.0%), MnO (av. 0.01%), MgO (av. 0.1%), CaO (av. 0.6%), Na_2O (av. 0.2%), K_2O (av. 0.4%) and P_2O_5 (av. 0.06%). All sandstone samples have more than 65% SiO_2, i.e. quartz-rich following the criteria of Crook, 1974, suggesting both mineralogical and chemical maturities. The variation of SiO_2 content (68.0 - 97.4%) between samples is related to variation in grain size and to severe corrosion by carbonate cement. The negative relationships between SiO_2 and each of TiO_2, Al_2O_3, Fe_2O_3, MgO, and K_2O (Fig. 7A) confirm that most of the silica is

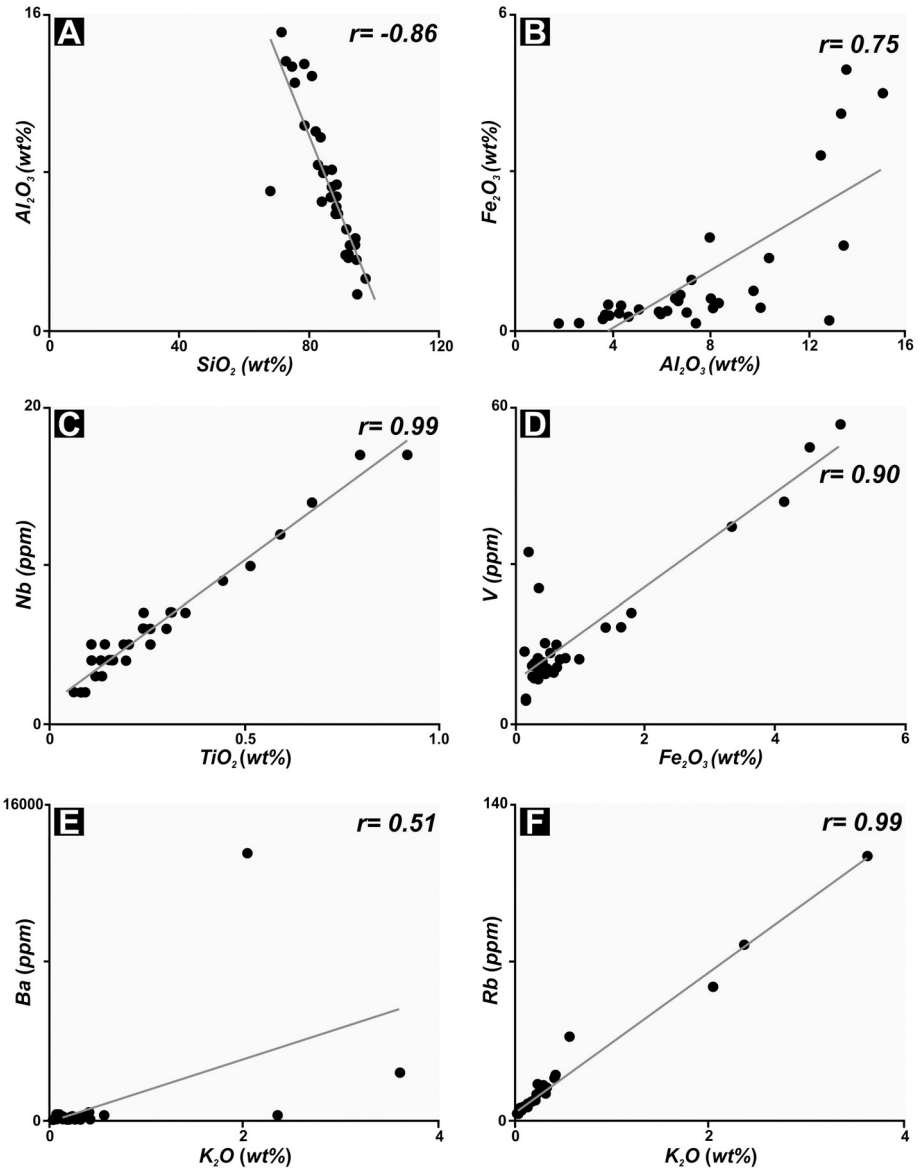

Fig. 7 Interrelationship examples between major and trace elements in the studied sandstones.

concentrated in quartz grains.

In contrast, most of the major elements are positively correlated with both Al_2O_3 and Fe_2O_3 implying that these elements are mainly associated with clay minerals and metal oxides. TiO_2 and Fe_2O_3 are positively correlated with Al_2O_3 (Fig. 7B), suggesting their association with phyllosilicates. According to Akarish and El-Gohary (2008), the concentration of K-bearing minerals has a significant influence on Al-distribution suggesting that the abundance of these elements is primarily controlled by clay content. However, a weak positive correlation (r = 2.4) is noted between Al_2O_3 and K_2O suggesting that significant proportions of the latter were removed during kaolinite formation from K-feldspar precursor.

The presence of CaO is probably related to diagenetic calcite cement that mostly dissolved to a great extent. The ratio of K_2O/Na_2O reflects the proportion of K-feldspar to plagioclase as well as the composition of feldspar themselves, and therefore, the decrease in the percentage of the unstable Na-feldspar can be taken as a mineralogical maturity (Sabaou et al., 2009). The detected high K_2O/Na_2O ratio (>>1; Table 3) is attributed to the common occurrence of K-bearing minerals such as K-feldspar, muscovite and illite compared to Na-plagioclases (Osae et al., 2006), as confirmed by petrographic study.

Trace elements

The Araba sandstones show a significant enrichment of barium (av. 607 ppm), strontium (av. 186 ppm) and zirconium (av. 217 ppm) compared to other trace elements (Table 3). The negative correlations between SiO_2 and trace elements suggest that most of the trace elements are concentrated in the clay mineral fraction. Nb and V are positively correlated with TiO_2 (r = 0.98 and 0.89, respectively; Fig. 7C), Al_2O_3 (r = 0.77 and 0.82, respectively), and Fe_2O_3 (r = 0.70 and 0.90, respectively; Fig. 7D), indicating that these elements are absorbed into phyllosilicates and/or associated with iron-oxide minerals. The transition elements such as Cr, Ni and V are well known to be concentrated in metal oxides (Turekian and Carr, 1960).

Ba is positively correlated with K_2O (Fig. 7E) suggesting that K-bearing minerals control its abundance (McLennan et al., 1983; Rahman and Suzuki 2007). Rb is very well correlated to K_2O (Fig. 7F). The coherent behavior of large cations (K, Ba and Rb) indicates that these elements are mainly concentrated in K-feldspar. Sr is mostly related to diagenetic calcite and partly incorporated from weathering of feldspars (Rahman and Suzuki, 2007), although no relation was found between K_2O and Sr. They generally show consistent trace elements relationships, as do high field strength elements (e.g. Zr, Nb and Y), indicating the chemical coherence and uniformity of the sediments (Rahman and Suzuki 2007).

Discussion

Provenance

The provenance of clastic rocks can be easily determined by several petrographical methods, including quartz typology (Young, 1976), rock fragment varieties (Pettijohn et al., 1987), and heavy mineral suites (Asiedu et al., 2000).

The high proportion of monocrystalline quartz grains in the Araba sandstones (Table 2) is attributed to the disaggregation of polycrystalline quartz during high energy and/or long distance transport from the source area (Dabbagh and Rogers, 1983). The dominance of unstrained over strained monocrystalline quartz grains points out to plutonic origin (Potter, 1978). Inclusions of bipyramidal zircon and prismatic microlites of tourmaline within quartz grains indicate derivation either from igneous or metamorphic rocks (Blatt et al., 1980; Morton et al., 1992). The dominance of polycrystalline quartz grains that are composed of two to five subcrystals and straight to slightly-curved intercrystalline boundaries point to a plutonic source (Blatt et al., 1980), whereas those with five or more elongated crystals with sutured and crenulated intercrystalline subcrystal boundaries and those with a bimodal distribution of crystal sizes suggest a metamorphic terrain derivation (Asiedu et al., 2000).

The scarcity of feldspar and rock fragments suggests that the source area underwent a long period of significant chemical weathering (Amireh, 1991). The exclusive occurrence of ZTR group indicates origination from plutonic igneous sources (Pettijohn et al., 1987) and points to prolonged abrasion and/or extensive chemical weathering (Avigad et al., 2005). Appling the diagram of Dickinson et al. (1983), the Araba sandstones are plotted in cratonic interior or recycled orogenic fields (Fig. 8). Such craton type reflects mature sandstones derived from relatively low-lying granitoid and gneissic sources that supplied from recycled sands of associated platform (Dickinson et al., 1983). Using the discriminant function plot after Roser and Korsch (1988), the Araba sandstones are exclusively plotted within field P4 (Fig. 9). According to Laird (1972), the sediments plotted in such fields are mainly derived from deeply weathered granitic-gneissic terrain, which are quartz-rich sandstones, poor in feldspar and rock fragments.

The general enrichment of SiO_2, greater than 70%; elevated K_2O/Na_2O ratio; high proportions of high field

strength elements (HFSE) such as Zr (av. 216 ppm), Ba (av. 607 ppm), Sr (av. 186 ppm) trace elements; and depleted concentration of transition elements such as Cr, Ni and V, as well as Fe_2O_3*+MgO (Table 3) suggest that the bulk of these sandstones were derived from felsic terrain such as granites and gneisses (Potter, 1978; Taylor and McLennan, 1985; Osae et al., 2006; Rahman and Suzuki, 2007; Akarish and El-Gohary, 2008).

Tectonic setting

Many authors have related sandstone geochemistry to specific tectonic setting (e.g. Bhatia, 1983; Blatt et al., 1980; Bhatia and Crook, 1986; Roser and Korsch, 1986; 1988). Even through diagenesis, that may alter the original chemistry; changes are themselves related to plate tectonic environment (Siever, 1979). Bulk composition should still reflect tectonic setting and hence enable development of chemically-based discriminants to supplement a petrographic approach (Roser and Korsch, 1986).

Petrographic examination of the Araba sandstones revealed the presence of: a) high proportions of quartz; b) predominance of monocrystalline quartz; c) more potash feldspar than plagioclase feldspar; and d) a paucity of rock fragments. These properties are consistent with the sediments deposited in passive continental margin environment (Crook, 1974; Potter, 1978; Taylor and McLennan, 1985). Crook (1974) proposed the use of quartz content to infer tectonic setting and linked quartz-rich (> 65% quartz) sandstones to passive (Atlantic-type) continental margins, intermediate quartz (15 - 65% quartz) sandstones to active (Andean-type) continental margins, and quartz poor (< 15%) sandstones to magmatic island arcs. The Araba sandstone is considered to be quartz-rich sandstone, thus corresponding to the Atlantic-type sandstone of Crook (1974).

The geochemical data obtained here are consistent with the average quartzarenite of Pettijohn (1963) and those of sandstones of Eastern Australia and NE Sinai (Table 4) that proposed to be deposited in a passive margin setting. However, various workers (e.g. Bhatia, 1983; Roser and Korsch, 1986; McLennan et al., 1990) have used the chemical composition of sandstones to discriminate tectonic settings. Roser and Korsch (1986) established a discrimination diagram using K_2O/Na_2O versus SiO_2 (Fig.

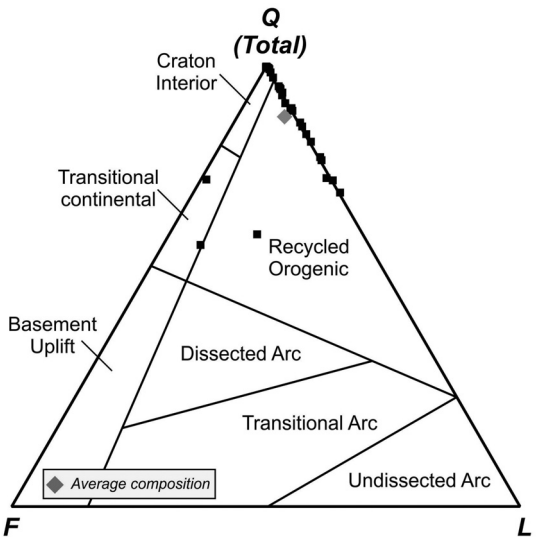

Fig. 8 QFL diagram after Dickinson et al. (1983).

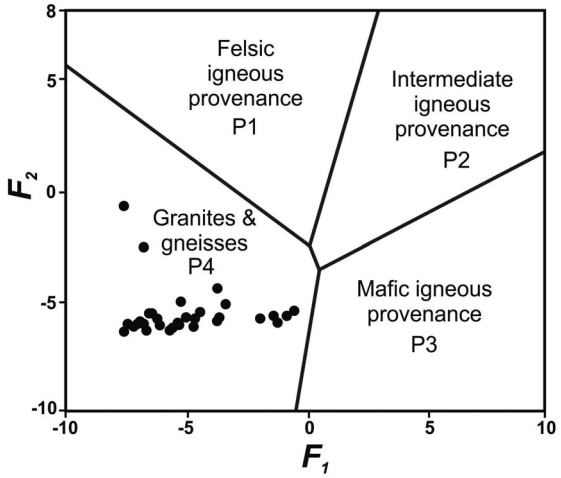

Fig. 9 Provenance discriminant function plot of the Araba sandstones (after Roser and Korsch, 1988). F1 and F2 refer to $-1.773TiO_2 + 0.607Al_2O_3 + 0.76Fe_2O_3^* - 1.5MgO + 0.616CaO + 0.509Na_2O - 1.224K_2O - 9.09$ and $0.445TiO_2 + 0.07Al_2O_3 - 0.25Fe_2O_3^* - 1.142MgO + 0.438CaO + 1.475Na_2O + 1.426K_2O - 6.861$, respectively.

Table 4 The average chemical composition of the Araba sandstones compared with other selected passive margin sandstones.

Oxides (Wt %)	1	2	3	4
SiO_2	96.6	87.8	84.1	89.6
TiO_2	0.2	0.3	0.5	0.3
Al_2O_3	1.1	8.1	8.4	7.8
Fe_2O_3	0.6	1.0	2.8	1.1
MnO	Nd	0.0	0.0	0.0
MgO	0.1	0.4	0.4	0.1
CaO	1.6	0.1	0.1	0.6
Na_2O	0.1	0.9	0.2	0.1
K_2O	0.2	1.3	3.5	0.4
P_2O_5	Nd	0.1	0.1	0.1
$Fe_2O_3^*$+MgO	0.6	1.5	3.1	1.2
Al_2O_3/SiO_2	0.0	0.1	0.1	0.1
K_2O/Na_2O	2.0	1.4	14.8	9.9
$Al_2O_3/(Na_2O+CaO)$	0.6	8.0	22.6	25.1

1: Average quartzarenite (Pettijohn, 1963); **2**: Cookman Suite, Eastern Australia (Bhatia, 1963); **3**: Lower Paleozoic sandstones, NE Sinai (Akarish and El-Gohary, 2008); **4**: Present study.

10) to determine the tectonic setting of terrigenous sedimentary rocks. Both SiO_2 and K_2O/Na_2O ratio increase from volcanic-arc to active continental margin to passive margin settings. On this diagram, the Araba sandstones plot exclusively in the field of passive margin (PM). In such a setting, the sediments are largely quartz-rich sandstones that derived from plate interior or stable continental areas and deposited in intra-cratonic basins or passive continental margins (Roser and Korsch, 1986). Maynard et al. (1982) used a similar plot of K_2O/Na_2O versus SiO_2/Al_2O_3 in their study of modern sediments to discriminate different tectonic settings. In their diagram, the present data are mainly plotted in the field of passive margin (PM) setting. Furthermore, plotting the data of chemical analyses on the discriminant function diagram (Bhatia, 1983) showed that the Araba sandstones fall within the passive continental margin (Fig. 11).

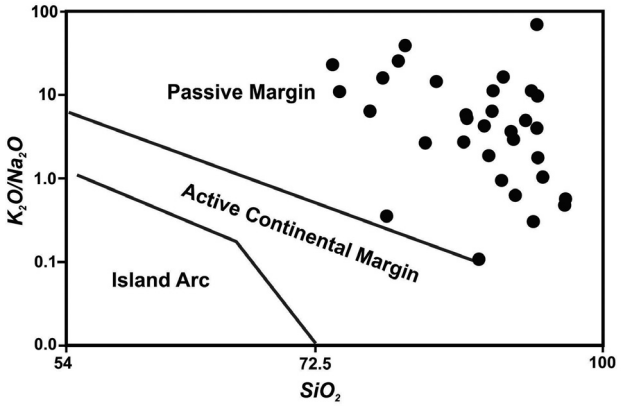

Fig. 10 Geochemical discrimination plot for the Araba sandstones (after Roser and Korsch, 1986).

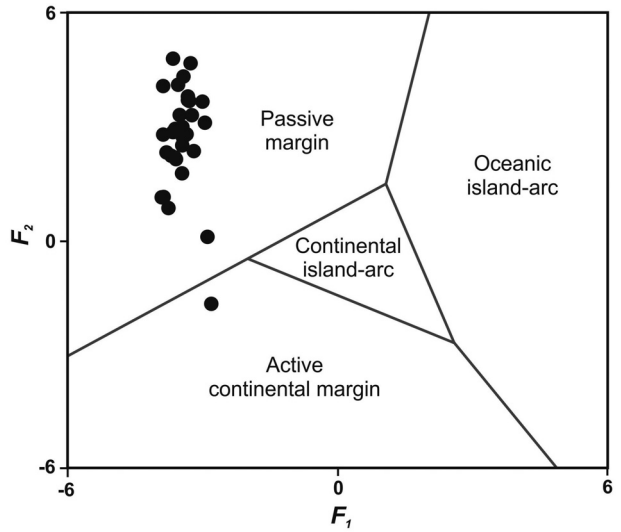

Fig. 11 Discriminant function diagram for the studied sandstones (after Bhatia, 1983). F1 and F2 refer to $-0.0447SiO_2 - 0.972TiO_2 + 0.008Al_2O_3 - 0.267Fe\neg_2O_3 + 0.208FeO - 3.082MnO + 0.14MgO + 1.95CaO + 0.719Na_2O - 0.032K_2O + 7.51P_2O_5 + 0.303$ and $-0.421SiO_2 + 1.988TiO_2 - 0.526Al_2O_3 - 0.551Fe_2O_3 - 1.61FeO + 2.72MnO + 0.881MgO - 0.907CaO - 0.177Na_2O - 1.84K_2O + 7.244P_2O_5 + 43.57$, respectively.

The studied sandstones are generally characterized by lower values of Fe_2O_3*+MgO, Al_2O_3/SiO_2, and TiO_2, as well as higher values of K_2O/Na_2O and $Al_2O_3/(CaO+Na_2O)$ (Table 3). Therefore, most of the samples are plotted within D field of Bhatia's (1983) diagrams (Figs. 12A and B). However, samples plotted within or close to field of active continental margin, are not consistent with the overall mineralogical composition and geochemical characteristics. According to Bhatia (1983) and Roser and Korsch (1988), passive margin sandstones usually exhibit variable composition. Their characteristics may overlap with those of active continental margin, but they can be distinguished by their enrichment in SiO_2 and K_2O/Na_2O ratio (>>1) and depletion in CaO, Na_2O, and TiO_2.

Chemical weathering/alteration

Alteration of igneous rocks during weathering results in depletion of alkali and alkaline earth elements and preferential enrichment of Al_2O_3 in sediments. Therefore,

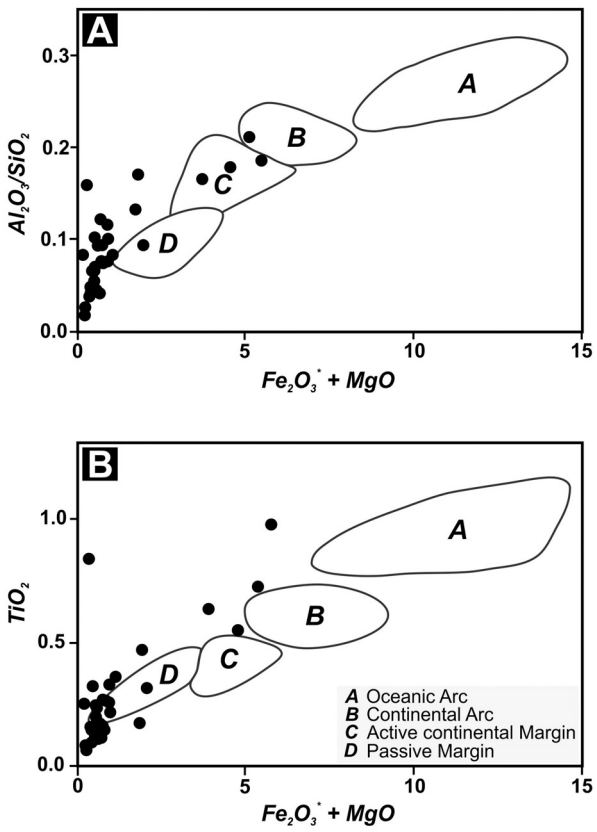

Fig. 12 A and B. Tectonic discrimination diagrams of the Araba sandstones (after Bhatia, 1983).

the weathering history of ancient sedimentary rocks can be evaluated in part by examining relationships among the alkali and alkaline earth elements (Nesbitt and Young, 1982). As the studied sandstones subjected to intensive alteration during post-depositional diagenesis, the term weathering is amalgamated with alteration to include the weathering effects at the source area plus the alteration of the sandstones during diagenetic processes.

A good measure of the degree of chemical weathering can be obtained by calculation of the Chemical Index of Alteration (CIA; Nesbitt and Young, 1982) and Plagioclase Index of Alteration (PIA; Fedo et al., 1995). High CIA and PIA values (i.e. 75 - 100) indicate intensive alteration as a result of removal of mobile cations (e.g. Ca^{2+}, Na^{+} and K^{+}) relative to the less mobile residual constituents (Al^{3+} and Ti^{+}), whereas low values (i.e. 60 or less) point to low incipient chemical alteration. The CIA and PIA are calculated in molecular proportions.

The calculated CIA and PIA values for the Araba sandstones vary from 44 to 99.3%, averaging 94%; and 42.4 to 99.97%, averaging 96.8%, respectively (Table 3). These higher values imply that, the present sandstones were subjected to intensive chemical weathering at the source area and/or extreme alteration and removal of alkali during diagenesis. The intensive chemical weathering in late Neoproterozoic-Cambrian times was supported by Beuf et al. (1971), who recorded the widespread occurrence of weathering profile that developed over Hoggar granites and below Cambro-Ordovician sandstone in the Algerian Sahara. In addition, the presence of paleosols and saprolite in southern Jordan (Selley, 1972) and Wajid area of south Saudi Arabia (Babalola et al, 2003) suggested that chemical weathering of the basement rocks was widespread in northern Gondwana at the beginning of the Paleozoic.

Meanwhile, the mineralogical maturity index (MI) that is expressed by the ratio of quartz to quartz + feldspar + rock fragments (cf. Bhatia and Crook, 1986; Mansour et al., 1999), ranges from 59.4 to 99.7%; av. 87.2% (Table 2), suggesting high mineralogical maturity. Figure 13 shows a good correlation (r = 0.7) between MI and CIA values suggesting that the chemical composition of the studied sandstones may be correlated, to a great extent, with the data of petrographic modal analysis.

The degree of chemical weathering can be addressed by the Al_2O_3-CaO+Na_2O-K_2O ternary diagram of Nesbitt and Young (1984). Unweathered rocks are clustered along the left-hand side of the K-feldspar-plagioclase join. Most of the studied samples are plotted away from the K-feldspar-plagioclase join line and close to Al_2O_3 apex (Fig. 14) indicating high degree of weathering and the preponderance of aluminous clay minerals within sandstones. The exceptionally high value of Na_2O in one sample is probably due to the presence of diagenetic halite cement rather than Na-rich feldspar (Table 2).

Paleoclimate

Climate affects sand composition through its destructive influence on parent rocks. To assess the paleoclimatic conditions affecting the Araba sandstones, the chemical maturity biplot of Al_2O_3+K_2O+Na_2O versus SiO_2 (Fig. 15), as well as the log/log plot of the ratio of

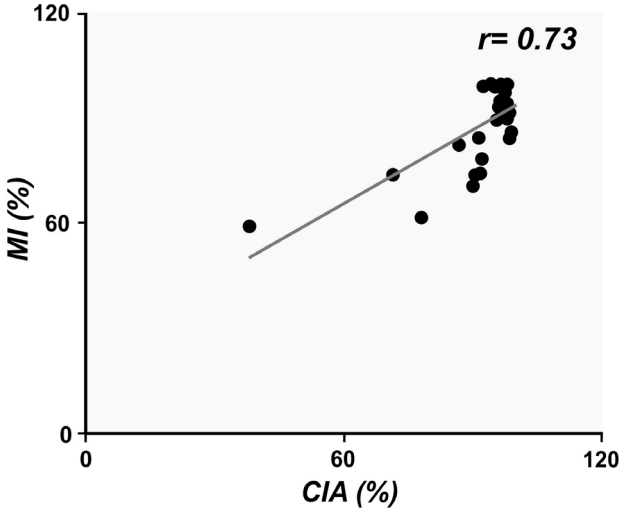

Fig. 13 Relationship between chemical index of alteration (CIA) and mineralogical maturity index (MI) of the Araba sandstones.

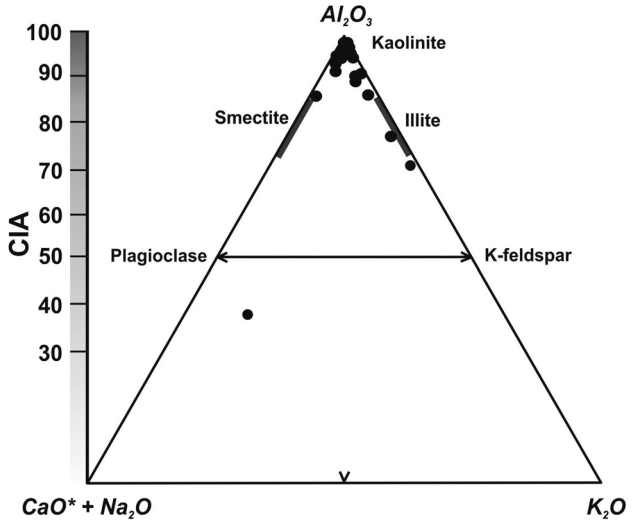

Fig. 14 Al_2O_3-Na_2O+CaO*-K_2O ternary diagram showing degree of alteration of the Araba sandstones (after Nesbitt and Young, 1984).

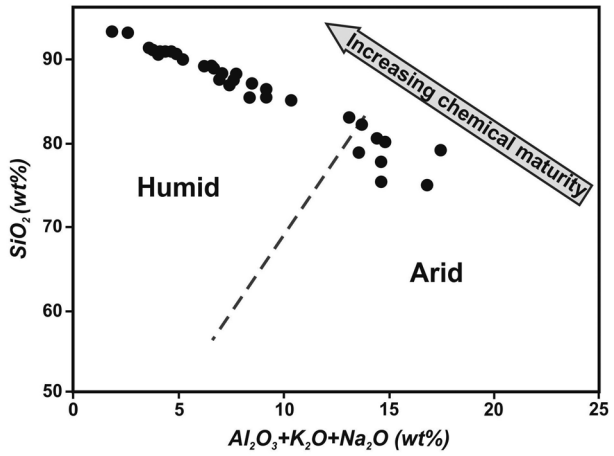

Fig. 15 Chemical maturity of the studied sandstones (after Suttner and Dutta, 1986).

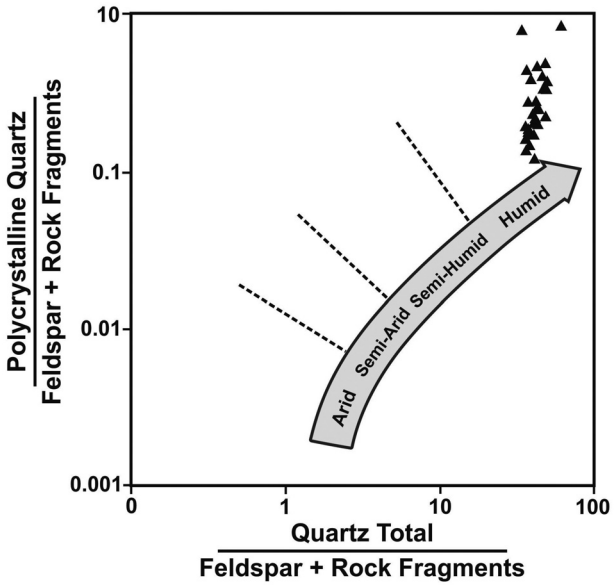

Fig. 16 Bivariant log/log plot of climatic condition of the studied sandstones (after Suttner and Dutta, 1984).

total quartz (Q) to total feldspar (F) plus rock fragments (L) versus the ratio of polycrystalline quartz (Qp) to total feldspar plus rock fragments (Fig. 16) given by Suttner and Dutta (1986) were used as a sensitive discriminator of sandstones with different climate heritage. The data showed that the detritus of these sandstones were mostly released under humid climatic conditions. This result is in harmony with the data obtained by Avigad et al. (2005) who attributed the mature Cambro-Ordovician siliciclastics to intensive chemical weathering of the Pan-African continental basement in warm-humid climate that prevailed over north Gondwana from the end of the Neoproterozoic to the Pre-glacial Ordovician time.

Conclusions

The Lower Paleozoic Araba Sandstone that was exposed in the northern Eastern Desert, Egypt, was petrographically and geochemically analyzed in order to document the provenance, tectonic setting, and role of chemical weathering. The sandstones framework grains are dominated by quartz followed by lithic fragments and feldspar together with muscovite mica and ZTR accessories. The sandstones are mostly quartz arenite in composition with frequent lithic arenite and rarely arkonic arenite. The study demonstrates that the sandstones were derived from the Precambrian basement complex of the Arabian-Nubian Shield and were deposited in a passive continental margin setting following the Late Pan-African Orogeny. The dominance of kaolinite clay mineral and elevated CIA and PIA values support concepts from earlier studies that these sandstones were affected by intensive chemical weathering under a warm-humid climate prevailed from the end of the Neoproterozoic to the end of Cambrian time.

Acknowledgements

This work is part of a Ph.D. project for the first author who is fully sponsored by the Japanese Ministry of Education, Culture, Sports, Science and Technology (MONBUKAGAKUSHO). We are grateful to Dr. Yoshimitsu Suda, Department of Geosciences, Osaka City University, for facilitating the use of geochemical instruments. We thank Prof. M. Kora (Mansoura University, Egypt) and Prof. A. Salem (Kafrelsheikh University, Egypt) for their helpful comments and constructive suggestions during the review of the manuscript.

References

Abdallah, A. M., Darwish, M., El-Aref, M. and Helba, A. A. (1992) Lithostratigraphy of the Pre-Cenomanian clastics of North Wadi Qena, Eastern Desert, Egypt. Geol. Arab World, Cairo Univ., 255-282.

Ahmed, S. M. and Osman, R. A. (1998) A field appraisal of sedimentary facies and environment of Pre-Carboniferous, SW Sinai, Egypt. Sediment. Egypt, 6, 21-32.

Akarish, A. I. M. and El-Gohary, A. M. (2008) Petrography and geochemistry of lower Paleozoic sandstones, East Sinai, Egypt: Implications for provenance and tectonic setting. J. Afr. Ear. Sci., 52, 43-54.

Alsharhan, A. S. and Salah, M. G. (1997)

Lithostratigraphy, sedimentology and hydrocarbon habitat of the Pre-Cenomanian Nubian Sandstone in the Gulf of Suez oil province, Egypt. GeoArabia, 2, 4, 385-400.

Amireh, B. S. (1991) Mineral composition of the Cambrian-Cretaceous Nubian series of Jordan: provenance, tectonic setting and climatological implications. Sediment. Geol., 71, 99-119.

Armstrong-Altrin, J. S., Lee, Y., Verma, S. P. and Ramasamy, S. (2004) Geochemistry of sandstones from the Upper Miocene Kudankulam Formation, Southern India: Implications for provenance, weathering and tectonic setting. J. Sedment. Res., 74, 285-297.

Asiedu, D. K., Suzuki, S., Nogami, K. and Shibata, T. (2000) Geochemistry of Lower constraints on provenance and Cretaceous sediments, Inner Zone of Southwest Japan: tectonic environment. Geochem. J., 34, 155-173.

Avigad, D., Sandler, A., Kolodner, K., Stern, R. J., McWilliams, M., Miller, N. and Beyth, M. (2005) Mass-production of Cambro-Ordovician quartz-rich sandstone as a consequence of chemical weathering of Pan-African terranes: Environmental implications. Ear. Plan. Sci. Let., 240, 818-826.

Babalola, L. O., Hussain, M. and Hariri, M. M. (2003) Origin of iron-rich beds in the basal Wajid Sandstone, Abha-Khamis Mushayt area, Southwest Saudi Arabia, Arab. J. Sci. Eng. 28, 3-24.

Barron, T. (1907) The topography and geology of the Peninsula of Sinai (Western Portion). Geol. Surv. Egypt, 241.

Beuf, S., Biju-Duval, B., de Charpal, O., Rognon, P., Gariel, O., Bennacef, A. (1971) Les Grès du Paléozoique Inférieur au Sahara: Sédimentation et Discontinités évolution structurale d'un Craton. Insitut Francais du Pétrol No 18, Editions Technip, Paris, 464.

Bhatia, M. R. (1983) Plate tectonics and geochemical composition of sandstone. J. Geol., 91, 611-627.

Bhatia, M. R. and Crook, K. W. (1986) Trace element characteristics of greywackes and tectonic setting discrimination of sedimentary basins. Contributions to Mineralogy and Petrology, 92, 181-193.

Blatt, H. (1992) Sedimentary petrology, 2nd ed., New York, 514 pp.

Blatt, H., Middleton, G. and Murray, R. (1980) Origin of Sedimentary Rocks, 2nd ed., Prentice-Hall, Englewood Cliffs, NJ.

Chaodong, W., Changsong, L., Yanping, S. and Xue, E. (2005) Composition of sandstone and heavy mineral implies the provenance of Kuga Depression in Jurassic, Tarin basin, China. Progress in Natural Sci., 15, 633-640.

Crook, K. A. W. (1974) Lithogenesis and geotectonics: the significance of compositional variation in flysch arenites (graywackes). Soc. Econ. Paleo. Min., Spec. Publ. 19, 304-310.

Dabbagh, M. E. and Rogers, J. J. (1983) Depositional environments and tectonic significance of the Wajid Sandstone of southern Saudi Arabia. J. Afr. Ear. Sci., 1, 47-57.

Dickinson, W. R., Beard, L. S., Brakenridge, G. R., Erjavec, J. L., Ferguson, R. C., Inman, K. F., Knepp, R. A., Lindberg, F. A. and Ryberg, P. T. (1983) Provenance of North American Phanerozoic sandstones in relation to tectonic setting. Geol. Soc. Am. Bull., 94, 222-235.

El Araby, A. and Abdel Motelib, A. (1999) Depositional facies of the Cambrian Araba Formation in the Taba region, east Sinai, Egypt. J. Afr. Ear. Sci., 29, 3, 429-447.

El Kelani, A. and Said, M. (1989) Lithostratigraphy of south eastern Sinai. Ann. Geol. Surv. Egypt, XVI, 215-221.

El Shahat, A. and Kora, M. (1986) Petrology of the Early Palaeozoic rocks of Um Bogma area, Sinai. Mansoura Sci. Bull., 13, 151-184.

Fedo, C. M., Nesbitt, H. W. and Young, G. M. (1995) Unraveling the effects of potassium metasomatism in sedimentary rocks and paleosols, with implications for paleoweathering conditions and provenance. J. Geol., 23, 921-924.

Furuyama, K., Hari, K. R. and Santosh, M. (2001) Crystallization history of primitive Deccan basalt from Pavagadh Hill, Gujarat, western India. Gondwana Res., 4, 427-436.

Ghandour, I. M., Tawfik, H. A., Abdel-Hameed, A. T. and Maejima, W. (2009) Facies analysis and sequence stratigraphy of the Cambrian Araba Formation, Somr El-Qaa'a area, North Wadi Qena, Egypt. Prog. and Abst., Ann. Meet. Sed. Soc. Japan, 31, 123.

Hardy, R. G. and Tucker, M. E. (1988) X-Ray Powder Diffraction of Sediments. In: Techniques in Sedimentology (Tucker, M. E. ed.), Blackwell Sci. Publ., London, 191-228.

Ingersoll, R.V., Bullard, T. F., Ford, R. L., Grimm, J. P., Pickle, J. D., Sares, S. W. (1984) The effect of grain size on detrital modes: A test of the Gazzi- Dickenson point-counting method. J. Sediment. Petrol., 54, 1, 103-116.

Issawi, B. and Jux, U. (1982) Contributions to the stratigraphy of the Paleozoic rocks in Egypt. Geol. Surv. Egypt, 64, 28.

Klitzsch, E. (1990) Palaeozoic. In: The Geology of Egypt (Said. R. ed.), Balkema, Rotterdam, 393-406.

Kora, M. (1991) Lithostratigraphy of the Early Paleozoic succession in Ras El-Naqb area, east central Sinai, Egypt. Newsl. Stratig., 24 , 45-57.

Laird, M. G. (1972) Sedimentology of the Greenland Group in the Paparoa Range, West Coast, South Island. N.Z.J. Geol. Geophys., 15, 372-393.

Mansour, A. M., Kurzweil, H. and Osman, M. R. (1999) Sedimentary nature of Nile sediments in Upper Egypt: Relationships and implications to weathering, climate of provenance. Sedimentology, 7, 37-54.

Maynard, J. B., Valloni, R. and Yu, H. (1982) Composition of modern deep sea sands from arc-related basins. Geol. Soc. London, Spec. Publ. 10, 551-561.

McCann, T. (1998) Sandstone composition and provenance of the Rotliegend and NE German Basin. Sediment. Geol., 116, 177-198.

McLennan, S. M., Taylor, S. R. and Eriksson, K. A. (1983) Geochemistry of Archean shales from the Pilbara Supergroup, Western Australia. Geochim. Cosmochim. Acta, 47, 1211-1222.

McLennan, S. M., Taylor, S. R., McCulloch, M. T. and Maynard, J. B. (1990) Geochemical and Nd-Sr isotopic composition of deep-sea turbidites: crustal evolution and plate tectonic associations. Geochim. Cosmochim. Acta., 54, 2015-2050.

McLennan, S. M., Hemming, S., McDaniel, D. K. and Hanson, G. N. (1993) Geochemical approaches to sedimentation, provenance and tectonics. In: Processes Controlling the Composition of Clastic Sediments (Johnsson, J. M. and Basu, A. eds.), Geol. Soc. Am., Spec. Pap., 284.

Moore, D. M. and Reynolds, R. C. (1989) X-ray diffraction and the identification and analysis of clay minerals. Oxford Univ. press, Oxford, 311-325.

Morton, A. C., Davies, J. R. and Waters, R. A. (1992) Heavy minerals as a guide to turbidite provenance in the Lower Paleozoic Southern Welsh Basin: a pilot study. Geol. Mag., 129, 573-580.

Nesbitt, H. W. and Young, Y. M. (1982) Early Paleozoic climates and plate motions inferred from major element chemistry of lutites. Nature, 299, 715-717.

Nesbitt, H. W. and Young, G. M. (1984) Prediction of some weathering trends of plutonic and volcanic rocks based on thermodynamic and kinetic considerations. Geochim. Cosmochim. Acta, 48, 1523-1534.

Osae, S., Asiedu, D. K., Banoeng-Yakubo, B., Koeberl, C. and Dampare, S. B. (2006) Provenance and tectonic setting of Late Proterozoic Buem sandstones of southeastern Ghana: Evidence from geochemistry and detrital modes. J. Afr. Ear. Sci., 44, 85-96.

Pettijohn, F. J. (1963) Chemical composition of sandstones, excluding carbonate and volcanic sands. In: Data of geochemistry (Fleischer, M. ed.), U.S. Geol. Surv. Prof. Pap. 440-S, 19.

Pettijohn, F. J., Potter, P. E. and Siever, R. (1987) Sand and Sandstone, 2nd ed., New York, Springer-Verlag, 533 pp.

Potter, P. E. (1978) Petrology and chemistry of modern big river sands. J. Geol., 86, 423-449.

Rahman, M. J. J. and Suzuki, S. (2007) Geochemistry of sandstones from the Miocene Surma Group, Bengal Basin, Bangladesh: Implications for Provenance, tectonic setting and weathering, Geochem. J., 41, 415-428.

Roser, B. P. and Korsch, R. J. (1986) Determination of tectonic setting of sandstone-mudstone suites using SiO_2 content and K_2O/Na_2O ratio. J. Geol., 94, 635-650.

Roser, B. P. and Korsch, R. J. (1988) Provenance signature of sandstone-mudstone suite determined using discriminant function analysis of major element data. Chem. Geol., 67, 119-139.

Sabaou, N., Ait-Salem, H. and Zazoun, R. S. (2009) Chemostratigraphy, tectonic setting and provenance of the Cambro-Ordovician clastic deposits of the subsurface Algerian Sahara. J. Afr. Ear. Sci., 55, 158-174.

Said, R. (1971) Explanatory note to accompany the geological map of Egypt. Geol. Surv. Egypt, 56, 123.

Said, M. and El Kelani, A. (1988) Contribution to the geology of southeast Sinai. In: 26th Ann. Meet. Geol. Soc. Egypt, Cairo, 30-31.

Salem, A. M., Abdel-Wahab, A. A. and McBride, E. F. (1998) Diagenesis of shallowly buried cratonic sandstones, southwest Sinai, Egypt. Sediment. Geol., 119, 311-335.

Seilacher, A. (1990) Palaeozoic trace fossils. In: The Geology of Egypt (Said, R. ed.), Balkema, Rotterdam, 649-670.

Selley, R. C. (1972) Diagnosis of marine and non-marine environments from the Cambro-Ordovician sandstones of Jordan, J. Geol. Soc., 128, 135-150.

Siever, R. (1979) Plate-tectonic controls on diagenesis. J. Geol., 87, 127-155.

Soliman, S. M. and El-Fetouh, M. A. (1969) Petrography of the Carboniferous sandstones in west central Sinai, Egypt. J. Geol., 13, 61-143.

Suttner, L. J. and Dutta, P. K. (1986) Alluvial sandstone composition and paleoclimate, I. Framework mineralogy. J. Sediment. Petrol., 56, 2, 329-345.

Tawfik, H. A., Ghandour, I. M., Abdel-Hameed, A. T. and Maejima, W. (2009) Impact of diagenesis on reservoir quality of the Cambrian Araba Sandstone in Gebel Somr El-Qaa area, west of the Gulf of Suez, Egypt. Proc. 6th Int. Sym. Geophy., Tanta Univ., Egypt, 9-33.

Tawfik, H. A., Ghandour, I. M., Maejima, W. and Abdel-Hameed, A. T. (2010) Reservoir heterogeneity in the Cambrian sandstones: A case study from the Araba Formation, Gulf of Suez Region, Egypt. J. Geosci., Osaka City Univ., 53, 1, 1-29.

Taylor, S. R. and McLennan, S. M. (1985) The Continental Crust: Its Composition and Evolution. Blackwell Sci., Oxford, 312 pp.

Tucker, M. (1988) Techniques in sedimentology. Blackwell, Oxford, 394 pp.

Turekian, K. K. and Carr, M. H. (1960) The geochemistries of chromium, cobalt and nickel. Inter. Geol. Cong., 1, 14-27.

Valloni, R. and Maynard, J. B. (1981) Detrital modes of recent deep sea sands and their relation to tectonic setting: a first approximation. Sedimentology, 28, 75-83.

Weissbrod, T. (1969) The Paleozoic of Israel and adjacent countries. Part 1: The subsurface Paleozoic of Israel. Bull. Geol. Surv. Isr. 47, 35.

Weissbrod, T. and Perath, I. (1990) Criteria for the recognition and correlation of sandstone in Precambrian and Palaeozoic-Mesozoic clastic sequence in the Near East. J. Afr. Ear. Sci., 10, 253-270.

Young, S. W. (1976) Petrographic textures of detrital polycrystalline quartz as an aid to interpreting crystalline source rocks. J. Sediment. Petrol., 46, 595-603.

Manuscript received August 30, 2010.

Revised manuscript accepted November 1, 2010.